Mango leaf disease classification using hybrid Coyote-Grey Wolf optimization tuned neural network model

J. Seetha[1] · Ramakrishnan Ramanathan[2] · Vishal Goyal[3] · M. Tholkapiyan[4] · C. Karthikeyan[5] · Ravi Kumar[6]

Abstract

The identification of diseases in plants contributes an important role in captivating disease control methods for the improvement of quality and quantity of crop yield. Mango trees are affected by different diseases and the identification of diseases is a tedious task till now when those diseases are manually detected. This paper proposes the novel hybrid Coyote Grey Wolf optimization (CO-GWO) algorithm for the classification of mango leaves as normal or diseased. The classification process is done through the extraction of significant features from the segmented image. The Neural network (NN) classifier performs the classification task, with the weights being adjusted using the proposed algorithm that acts a major role in the enhancement of the classification accuracy. The effectiveness of the proposed model is evaluated concerning the evaluation metrics, namely accuracy, precision, recall, and F1 measure, and is attained to be 96.7111%, 97.5712%, 97.1504%, and 96.4792%, respectively. This shows the superiority of the proposed technique in the effective classification of mango leaf classification as compared with the existing techniques.

✉ J. Seetha
seetha.vital@gmail.com

1   Department of Computer Science Engineering, SRM Institute of Science and Technology, Chennai 600089, India

2   Department of IT, Technology & Research (Deemed to Be University) Vadlamudi, Vignan's Foundation for Science, Guntur District, AP, India 522213

3   Department of ECE, GLA University, Mathura, Uttar Pradesh, India

4   Department of Civil Engineering, Saveetha School of Engineering, Saveetha Institute of Medical and Technical Sciences (SIMATS), Chennai, Tamil Nadu 602105, India

5   Department of Computer Science Engineering, Koneru Lakshmaiah Education Foundation, Deemed to Be University, Guntur, AP 522502, India

6   Department of ECE, Jaypee University of Engineering and Technology, Guna 473226, India

Springer

1 Introduction

Plant diseases are the primary cause of agricultural output quality and quantity losses all over the world. These losses have a negative impact on the costs of production and incomes of all agricultural stakeholders [1]. However, equipment is scarce for quick and reliable identification. If an epidemic strikes, the well-being and livelihood of farmers, as well as the country's food supply and nutritional security, are all at risk [2]. Mango trees are important for biodiversity and provide a variety of fruits. Mango is a popular fruit crop in India, and it contributes significantly to the country's economy [3]. With 13.79 million tons of wheat produced, India produces roughly half of the world's wheat [4]. As a result, global awareness of mango plant cultivation as a means of increasing fruit output through sustainable agricultural practices is expanding [5]. Mango plant disease, on the other hand, is a major hindrance to growing enough fruits to meet public demand [6]. Mango malformation disease, Anthracnose, Bacterial flower disease, Golmachi, Moricha disease, Shutimold, Bacterial black spot, Apical bud necrosis, Red rust, Lichens, Powdery mildew, Root rot and damping off, Ganoderma root rot are just a few of the illnesses that can damage mango plants [7].

Pathogens, such as bacteria, viruses, fungi, parasites, and even unfavorable environmental circumstances can cause such diseases [8]. The photosynthetic process is impaired by leaf disease, which results in plant death. The type of disease is determined by the symptoms and the afflicted leaf area. Identifying plant illnesses used to be done by farming specialists for checking plants regularly. Small farms have an easier time identifying illnesses and taking urgent preventative management actions [9]. However, it is time intensive and costly in the case of large farms. It is critical to identify illnesses in the early stages because early detection of plant diseases allows us to minimize damage, lower production costs, and increase revenue [10]. Many times, human intelligence alone is ineffective in identifying the exact ailment. Farmers used to follow specialists' observations of diseased plants, or experts would come to the farm and provide advice to the farmers, who would then take the required precautions to safeguard the plant from disease [11]. Finding a reliable expert becomes tough, and the approach does not function well for big sectors; in addition, such a procedure normally takes a long time. This strategy is also costly because it necessitates ongoing monitoring for accurate and prompt farm identification.

As a result, illness detection methods that are quick, automatic, low-cost, and accurate are needed. Diseases in agricultural goods are caused mostly by two types of organisms: live and nonliving. Bacteria, insects, fungi, and various viruses are living agents, whereas non-living agents include excess wetness, temperature changes, fewer nutrients, insufficient lighting, and various contaminants [12]. Many applications for leaf identification, lead disease detection, fruit disease detection, and other agricultural applications have been developed [11]. As a result, finding an autonomous, accurate, rapid, and less expensive plant disease identification technique is critical [13]. Artificial intelligence includes machine learning as a subset. It focuses on system design, learning, and prediction based on previous experience. Data collection begins the learning process, comparable to personal experience, to look for data trends. Machine learning-based techniques have recently been utilized to detect disease in plants, where photos are taken and processed to acquire the data needed for analysis. Several recent techniques related to mango leaf disease classification include Ensemble Stacked Deep Neural Network (ESDNN) [14], Hybrid Deep Learning with Support Vector Machine (HDL-SVM) [15], Optimized Recurrent Neural Network (ORNN) [16], Lightweight Convolutional

Neural Network (LCNN) [17], Deep Convolutional Generative Adversarial Networks (DCGAN) [18], Convolutional Neural Network (CNN) [19], etc., are developed to predict the mango leaf infection accurately. However, these state-of-art approaches are effective in predicting leaf diseases and their reliability depends on the quality and quantity of the training database. Moreover, these techniques face issues like overfitting, model complexity, and lack of generalization capacity. Hence, a novel hybrid CO-GWO was proposed in this article to overcome the issues and challenges in the existing techniques.

The basic idea behind this research is to provide an acceptable and effective approach for classifying the mango leaf disease, as well as to encourage the use of appropriate mechanisms for finding early and cost-efficient solutions to the problem. Computer vision and deep learning processes have been prominent in the classification of numerous fungal illnesses due to their superior computation and accuracy. As a consequence, this paper introduces a hybrid optimization algorithm, named CO-GWO algorithm for the classification of mango leaf disease. The classification of mango leaf disease is done through the NN classifier, the weights of which are optimally tuned using the proposed CO-GWO algorithm. The significant features, such as Local Binary pattern (LBP), Local Directional Pattern (LDP), and Local optimal-oriented pattern (LOOP) are extracted from the pre-processed image to make the classification process effectual. This research provides a detailed elucidation of the proposed model, and with the results, the efficacy of the proposed classification model can be validated. In addition, a comprehensive analysis is provided based on the performance of conventional classification strategies to analyze the superiority of the proposed method of mango leaf classification.

1.1 The important contribution of the article is

- The proposed method creates an automated strategy, named novel hybrid CO-GWO-NN for the recognition of the disease in mango leaves.
- This proposed study gives enhanced accuracy for making a deep observation over different models of NN.
- The accuracy of the proposed model is good enough as compared to other methods due to the implementation of transfer learning over the classes.
- This proposed model is exposed in such an effective way that makes it more competitive than the conventional models of mango leaf disease classification.

The remaining of this paper is organized as follows: Section 2 presents the survey of the recent strategies of mango leaf disease classification with the challenges associated with them. Section 3 describes the architecture of the NN model and the implementation of mango leaf disease identification using the proposed CO-GWO-NN model, followed by the results of this work in Section 4. Section 5 deals with the conclusion.

2 Motivation for the research

This section deliberates the survey of the conventional methods of mango leaf disease classification with their challenges in detail.

2.1 Literature survey

The methods for performing disease classification in mango leaves described in this part are as follows: Rasel Mia et al. [20] introduced a Neural Network Ensemble (NNE) for Mango Leaf Disease Recognition (MLDR). The goal of this study was to employ machine learning to detect indications of plant diseases faster than a manual monitoring system. It would also save time to diagnose disease using a machine rather than the old method, which would aid in the proper treatment of mango leaf disease. However, texturing and color characteristics are ignored, which has an impact on recognition accuracy. Arivazhagan and VinethLigi [21] devised a deep learning-based method for detecting leaf illnesses in Mango plant species. The model got better at detecting leaf diseases in mango trees, indicating that it may be utilized in real-time applications. Finding the appropriate parameters for a CNN model, on the other hand, is still a research topic. Ray AdderleyJmGining et al. [22] wanted to use image processing to create a recognition system that could detect the presence of illness in mango leaves. With a better level of precision, the system accurately detects and diagnoses the condition. The collected image may be too complex for the system to analyze, especially during the segmentation step, if the camera was not properly positioned.

Through the CNN approach, Aditya Raj Bongshi et al. [23] concentrated on categorizing and differentiating the illnesses of mango leaves. The findings of this study showed that using a CNN to generate illness-differentiating proof from an image is a good technique for high-accuracy automated mango disease distinguishing verification. The method, on the other hand, does not focus on additional diseases and must be improved to perform such tasks. SanathRao et al. [24] used a dataset of 8,438 photos of damaged and healthy leaves gathered from the Plant Village dataset and captured locally to detect and diagnose Mango leaf illnesses. Even though deep learning is a popular model for detecting diseases, further improvement is required due to specific restrictions in the field of research. Rabia Saleem et al. [10] developed a new segmentation strategy for segmenting the diseased part with the consideration of the vein model of the leaf, from which the classification process is executed using the Support vector machine (SVM) classifier. The model was very useful to mango plant growers for the appropriate and timely identification and recognition of diseases. However, the model was capable to work only for less data in the dataset. Rama Koteswara Rao and Swathi [25] employed an SVM algorithm to detect the disease of mango leaves. The developed system was excellent in computation and simple, but for large fields the procedure is time-consuming.

2.2 Challenges

The challenges possessed by the techniques of mango leaf disease classification are enlisted below:

- Automated identification of diseases in mango plant leaves is still a dispute as disease detection by manual means is not a practicable option in this automated era because of its increased cost and the non-availability of mango specialists and the changes in the indications [10].
- Many sophisticated technologies in modern agricultural models are developed to work constantly and need human involvement or regular screening to avoid errors. Not only

the devices are costly, but also possess an inadequate range of applications and adaptability in use [26].

- It is difficult to establish appropriate parameters in SVM if the training data is not linearly separable, which is one of its shortcomings [20].
- The perception and hand method looks less proficient as it uses more time, and the farmers may ignore some leaves that are previously affected and fail at the right time to prevent and take care of them [22].

3 Proposed model of disease classification in mango leaf

The detection of diseases in leaves has been a long research area for the past few decades. Classification of mango plant disease by its leaf observation is dependent on cost of the crop loss and plant populations. The method must be cost-effective and user-friendly, and one must possess the basic biological procedures of the plant. This is also used in the evaluation of crop cover, biocides, biosecurity, and claims. Image processing acts as one of the low-priced methods to recognize the disease using the RGB feature [23]. It is used to enumerate the diseased area, size, and nature of the leaves and also to find the edges of the affected area.

A novel hybrid optimization tuned NN model is proposed in this paper to classify the mango plant leaf diseases. The schematic depiction of the proposed model is depicted in Fig. 1. In the initial step, the leaf images are extracted from the dataset, and the extracted
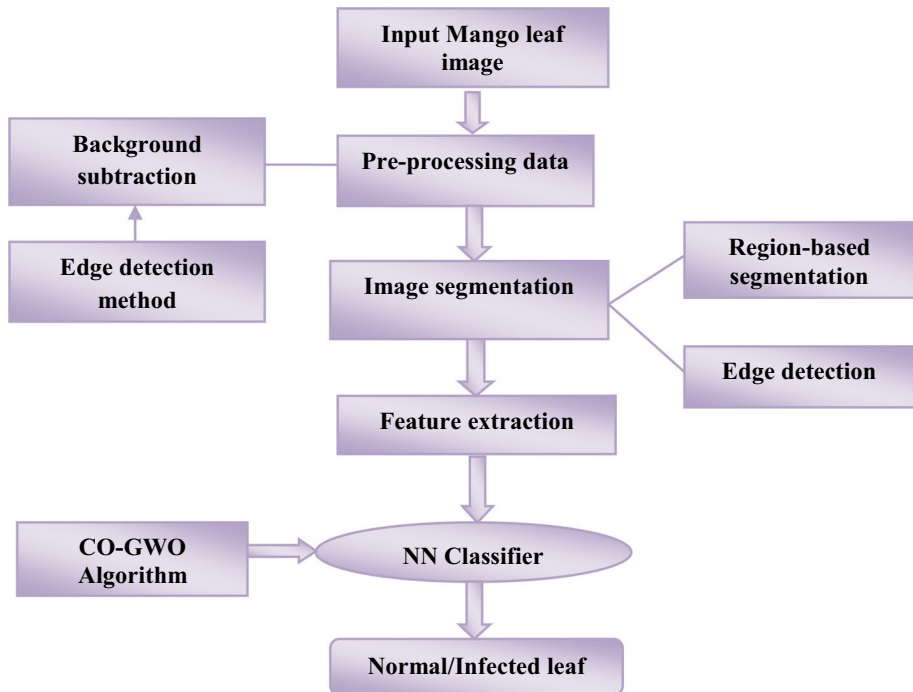

Fig. 1 Block diagram of a proposed classification model

images are subjected to pre-processing for removing the background of the input image. Then, the proposed hybrid optimization tuned NN model involves in the classification process to identify the image either as the normal image or as a diseased one. The weights of the NN are optimally tuned using the proposed GO-GWO algorithm which assists in the enhancement of the classification accuracy of the proposed model.

3.1 Input mango leaf image

The analysis of mango leaf image is crucial in agricultural applications, due to the needs associated with it in enhancing the detection accuracy of the proposed classification module. The classification of mango plant disease begins with the collection of plant leaf images. The input database contains images of both the healthy and the infected mango leaves. Moreover, the collected images are labeled as different classes such as normal or infected disease types. These images act as the input for the classification process. This image database acts as the input for the Neural Network classifier. The input dataset is mathematically represented as,

$$M = \{m_p\};(1 \leq p \leq g) \tag{1}$$

where, g refers to the total images of the input dataset and m_p is the pth image of the input dataset. The input images extracted from the dataset are processed in such a way as to perform the classification process in the proposed research.

3.2 Image pre-processing

Preprocessing leaf images previous to extraction and categorization is a typical technique. Different pre-processing strategies can be used to reduce noise from the attained photographs. These images may have an undesired background, which affects the prediction accuracy. As a result, the background of the original image must be eliminated before feeding the images to convolutional layers. The edge detection method is utilized to remove the background in this paper. This method is used at the strongest line in the middle of the symmetrical leaf which indicates the leaf's primary vein. The secondary veins are the straight lines that are followed near the vein. The edges of the leaf are joined to form the leaf's boundary after the secondary veins have been discovered. The counters are converted to polar coordinates using the centroid of the primary vein [26].

$$Y = ax^3 + bx^2 + cx + d \tag{2}$$

Coefficients of a three-degree polynomial in the least squares sense are approximated to match the smooth data as expressed in Eq. (2). The curve is extracted, and the appropriate part is extracted, removing the image's background.

3.3 Image segmentation

Image segmentation is a strategy for making a picture more meaningful and understandable. The technique of separating an image into many pieces depending on its qualities or likeness is referred to as segmentation. Different segmentation algorithms, such as k-means clustering, changing the RGB image in the model, and so on, can be applied. Dividing the image, or any relation, into different segments with similar features is of more concern

[22]. The division is twofold in the applications of plant disease recognition. The first element of the section is to get rid of the ailment-affected leaf's foundation. The second part of the split is to distinguish between disease-affected tissues and solid tissue. The two splits, such as edge detection and region-based concept are used to complete the division. Edge Detection is used to recognize the discontinuity between the leaf and the image's surroundings, edges are determined. Pixels that are associated with a specific item are grouped into region-based concepts. At any pace, one pixel is associated with the area in each phase and is considered over.

3.4 Feature extraction

The next significant step in the proposed mango leaf disease classification module is the extraction of the significant features from the input mango leaf images obtained from the dataset. The feature extraction strategy is used to develop the feature vector from a regular vector. The extraction of the feature acts as an important task in image processing, and is applied in various areas of image processing. Color, morphology, and texture can be taken as a feature for the detection of leaf disease. In other words, a feature is an idiosyncratic determination that is extracted from the input images in the proposed classification module. It involves selecting the features or data that are most significant to execute the classification process. The features that are needed to be extracted in the proposed system are the LDP, LBP, and LOOP features.

3.4.1 Local binary pattern

LBP is a basic yet efficient texture operator that identifies the pixels of the picture by calculating the threshold of each pixel's neighborhood and outputs a binary value [27]. The LBP records the variation patterns relating to the image's intensity and has the image's discrimination properties. The value of LBP can be calculated as follows:

$$LBP\left(r_n, s_n\right) = \sum_{q=1}^{7} \alpha\left(I_q - I_n\right) 2^q \tag{3}$$

$$\alpha\left(I_q - I_n\right) = \left\{ \begin{array}{c} 1, \ if \ \left(I_q - I_n\right) \geq 0 \\ 0 \ Otherwise \end{array} \right\} \tag{4}$$

where, I_n is the intensity of the image A, at the pixel $\left(r_n, s_n\right)$, and $I_q(q = 1, 2, \dots, 7)$ is the pixel intensity in the 3×3 neighborhood of $\left(r_n, s_n\right)$, except the center pixel I_n.

3.4.2 Local directional pattern

When compared to LBP, the local directional pattern [28] is a robust feature commonly employed for image processing that provides better results. To encode the picture texture, the LDP assesses the edge response value with different orientations. Edge responses are less vulnerable to noise and depict the natives, such as different sorts of curves, corners, and junctions. As a result, the pixel intensity is determined by the gradient magnitude of surrounding pixels. The benefit of LDP is examined and applied in the planned pest detection study. The LDP value for each pixel $\left(r_n, s_n\right)$ in the image A is calculated as follows,

$$LDP(r_n, s_n) = \sum\nolimits_{q=1}^{7} \alpha(\beta_q - \beta_\gamma) 2^q \tag{5}$$

$$\alpha(\beta_q - \beta_\gamma) = \left\{ \begin{array}{cc} 1, & if\ (\beta_q - \beta_\gamma) \geq 0 \\ 0 & Otherwise \end{array} \right\} \tag{6}$$

where I_q is the pixel of intensity with $(q = 1, 2, \ldots, 7)$ and is the eight responses of the Kirsch masks, with $(q = 1, 2, \ldots, 7)$.

3.4.3 Local optimal-oriented pattern

LOOP is defined as the non-linear joining of both LBP and LDP for handling the disadvantages of the LDP and LBP techniques [29]. The LOOP idea is used to overcome limitations such as LBP's wrong binary value and LDP's self-imposed restrictions. For the image A, the LOOP value at the pixel (r_n, s_n) is calculated as follows,

$$\text{LOOP}(r_n, s_n) = \sum\nolimits_{q=1}^{7} \sum\nolimits_{q=1}^{7} \alpha(I_q - I_n) 2^{\varpi q} \tag{7}$$

$$\alpha(I_q - I_n) = \left\{ \begin{array}{cc} 1, & if\ (I_q - I_n) \geq 0 \\ 0 & Otherwise \end{array} \right\} \tag{8}$$

The LOOP descriptor, which cancels the empirical assignment of the LDP parameter value, encodes rotation invariance in the main formulation. The feature vector is thus developed using the combination of the three features, such as LBP, LDP, and LOOP, and is represented as $F_{\text{Vector}} = \{F_{LBP}, F_{LDP}, F_{LOOP}\}$. The feature vector thus formed acts as the input to the proposed CO-GWO-NN model to execute the classification process.

3.5 Neural network classifier in mango leaf classification

The categorization between normal and diseased mango leaves can be made using ML algorithms, which automatically detect the presence without the need for human intervention. When compared to other machine learning techniques, the answers acquired using neural networks have several advantages in a variety of applications. The NN is a mathematical model based on the biological NN, which is made up of a linked collection of artificial neurons that uses a connection technique to calculate information. The NNs are computing models with a huge number of interconnections and simple processors that are extremely parallel. The main premise for the construction of NN is human features, and it has neuron layers to process the data that is provided as input. The data flow is represented by multiplying the NN's input with the weights [30]. The weights are evaluated by the mathematical functions, which then provide the neuron's activation function. The output of the NN can be adjusted as expected with the proposed hybrid CO-GWO optimization algorithm's optimal weight tuning. Figure 2 depicts the structure of the NN.

The output of the ANN can be mathematically expressed as,

$$O_{NN} = C\left(\sum\nolimits_{NN=1}^{o} W_{eNN} i_{NN} \right) + bias \tag{9}$$
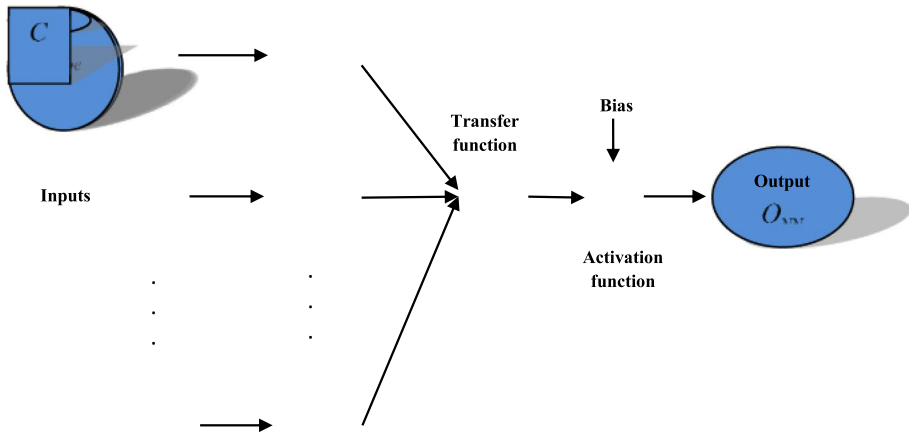
Fig. 2 Structure of neural network

where C represents the activation function, i_{NN} is the input, and W_{eNN} indicates the weight measures. The classification of the mango leaf either as normal or diseased is performed using the NN classifier. The advantage of using NN [31] is that the classifier automatically performs the classification task without the need for humans to intervene. The accuracy of categorization relies on the proper tuning of the hyper-parameters of the NN classifier using the proposed hybrid CO-GWO optimization algorithm.

3.6 Proposed hybrid CO-GWO optimization algorithm

The proposed CO-GWO optimization algorithm is a hybrid meta-heuristics, proposed through hybridizing the features, like the social dominance features and the hierarchy-based hunting features [32] of the Canidae family. The standard optimizations exhibit features focused on hunting behaviors, which announces a dynamic nature in handling convergence issues. The proposed CO-GWO algorithm solves this issue through the dynamic features of the population in the Canidae group, which boosts the ability of the proposed algorithm to attain better global optimal convergence as compared to basic optimization techniques that often converge to the local optimal solutions with better stability among exploitation and exploration phases.

3.6.1 Motivation of proposed optimization algorithm

The social dominance and hierarchy-based hunting skill of the coyotes and the social hunting hierarchy features of the grey wolf are incorporated to exhibit the functional modalities of the hybrid meta-heuristics, which is a population-based optimization. The population considered in this optimization belongs to the family Canidae, and they live in groups. The hierarchy-based hunting phenomenon exhibits a hunting hierarchy with the presence of grey wolfs, such as leading grey wolf, representative grey wolf, obeyer grey wolf, and scapegoat grey wolf, where the hierarchy-based hunting experience and the social hunting hierarchy features of the grey wolfs ensures the effective convergence. As stated above, the hierarchy-based hunting experience of the population is supported by the hierarchical levels, where the leading grey

wolf lies on the top-most level of the hierarchy and is responsible for creating solutions concerning resting, hunting, and so on.

The leading grey wolf instructs the other grey wolf during hunting, while the leading grey wolf is not the strongest over other grey wolfs and does not at all mate within the group, but stays as the best grey wolfs over the group of grey wolfs. The representative grey wolf lies on the second level in the order as it instructs the leading grey wolf by transferring the resolution to the subordinate grey wolf in the search area. The scapegoat grey wolfs remain in the lowest level, protecting the whole strength. The obeyer grey wolfs lie just over the scapegoat grey wolf, and principally, remains for the orders from the leading grey wolf. The major phases in the proposed CO-GWO algorithm are,

1) Social tracking hierarchy
2) Surrounding phase
3) Grey wolf's hunting phase
4) Social dominance stage
5) Exploration stage

The novel hybrid CO-GWO algorithm, based on the hierarchy-based hunting experience of the coyotes and the social hunting hierarchy features of the grey wolfs are mathematically modeled as below,

3.6.2 Mathematical design of proposed CO-GWO optimization

The mathematical representation of the grey wolfs in the various stages is summarized in this section as described below,

a) Social tracking hierarchy: The order of the grey wolfs pursues the leading, representative, obeyer, the scapegoat grey wolfs with the leading grey wolf being the strongest among the entire grey wolfs. The representative and the obeyer grey wolf pursue the second and third position in the order and are considered as the second and third best grey wolf, respectively, while remaining the grey wolf's strength stays as the scapegoat grey wolfs.

b) Surrounding phase: In this phase, the grey wolf environs the prey depending on the grey wolf's need and convenience. The grey wolf in the surrounding phase is modeled as,

$$J_{kl}^{t+1} = J_L^t - H.z \tag{10}$$

where, J_{kl}^{t+1} indicates the position of a kth grey wolf at l^{th} the coordinate axis and $t + 1$ represents the updated location. Let J_{kl}^t indicates the location of the prey, z is the remoteness among the prey and the grey wolf, and H is the coefficient vector. The distance vector is formulated as,

$$z = \left| U_1.J_L^t - J^t \right| \tag{11}$$

where, J^t represents the position of a grey wolf at time t and U_1 indicates the coefficient vector. The coefficient vectors $H\ U_1$ are mathematically modeled as,

$$H = 2V.w_1 - V \tag{12}$$

$$U_1 = 2w_2 \tag{13}$$

where V gradually decreases to 0 from 2 with the number of iterations w_1 and w_2 indicates the random vector that ranges between 0 and 1.

c) Grey wolf's hunting Phase: The grey wolf can identify the prey, where the process of hunting is done using the leader grey wolf, where the representative grey wolf and the obeyer grey wolf involve in the hunting act. The general grey wolf features are expressed as,

$$z_L = |U_1 J_L - J| \tag{14}$$

$$z_M = |U_2 J_L - J| \tag{15}$$

$$z_T = |U_3 J_T - J| \tag{16}$$

where, z_L, z_M, z_T indicates the current path of the best grey wolf at the time of hunting. $U_1, U_2,$ and U_3 represents the random constraints of the grey wolfs that balance between the exploration and exploitation phases. The prey is surrounded by the grey wolfs, while the location of the prey stays nearer to the grey wolfs. At this step, the instruction is formulated by the leading grey wolf based on which the representative grey wolf orders the other grey wolfs to trap the prey. The distance vectors are formulated as,

$$J_1 = J_L - H_1 z_L \tag{17}$$

$$J_2 = J_M - H_2 z_M \tag{18}$$

$$J_3 = J_T - H_3 z_T \tag{19}$$

where, $H_1, H_2,$ and H_3 represents the coefficient vectors, and J_L be the best solution at the time t. $H_1, H_2,$ and H_3 indicates the tunable parameters in the optimization process that takes charge of the optimal convergence by guiding to the local optimal solution, while improving the convergence to a global optimal solution. In general, the process of hunting among the grey wolfs relies on the first three best solutions based on leader, representative, and obeyer grey wolfs [17] concerning their positions as,

$$J_{kl,V}^{t+1} = \frac{J_1 + J_2 + J_3}{3} \tag{20}$$

where J_1 indicates the location of the leader grey wolf, J_2 represents the location of the representative grey wolf, and J_3 indicates the position of the obeyer grey wolf of the optimization procedure, referring to the first three best locations of hunting. It is clear from the above modeling that the hunting is guided by the remoteness among the grey wolf and the prey, and the tunable coefficient parameters. The hunting procedure and the rate of convergence are improved with the consideration of the hierarchy-based hunting experience of the grey wolfs [33]. The solution highlighting the hierarchy-based hunting features is mathematically expressed as,

$$J_X^{t+1} = J_4 = J_X^t + h_1 D_1 + h_2 D_2 \tag{21}$$

where, J_X^t is the location of the Xth grey wolf at t^{th} iteration, h_1 and h_2 are the random parameters that vary from 0 to 1. The term D_1 represents the alpha influence and the

term D_2 indicates the pack influence. The integration of the hybrid features thus given by,

$$J_{kl,V}^{t+1} = \frac{J_1 + J_2 + J_3 + J_4}{4} \qquad (22)$$

Thus, we obtain,

$$J^{t+1} = \left[\frac{(J_L + J_M + J_T) - (H_1 z_L + H_2 z_M + H_3 z_T) + (J_X^t + h_1 D_1 + h_2 D_2)}{4} \right] \qquad (23)$$

Equation (23) is the updated expression of the CO-GWO optimization algorithm, which relies on the constraints achieved from the social prevalence and hierarchy-based hunting features along with the social hunting hierarchy features of the grey wolfs. The proposed CO-GWO optimization algorithm possesses enhanced achievement of the global best solution through Eq. (23).

d) Social dominance stage: In this phase, the grey wolfs engage in probing the prey only inside the search area and it chooses the local best areas to assault the prey and complete the hunting procedure that is precisely formulated concerning H varying between the intervals $-2w_1$ to $2w_1$. Here, the value w_1 deteriorates to 0 from 2 with the increase in iterations. The revision of the location depends on the social hunting hierarchy of the grey wolfs with fulfilling the condition H < 1.

e) Exploration stage: In this phase, the grey wolf, such as leader, representative, obeyer, and the scapegoat explores the exterior to the resolution space, and ends at the global best possible outcome. The exploration stage fulfills the criterion |H > 1|, which is managed by the factor U to assure enhanced hunting features. The proposed CO-GWO optimization algorithm offers a better balance among the exploitation and exploration phases thereby, avoiding the local optimal solutions to generate a global best outcome.

3.6.3 Algorithmic procedure of CO-GWO optimization

The step-wise rationalization of the CO-GWO optimization is stated below:

i) Initialization: In this phase, the grey wolf population was initialized, in which each grey wolf represents the hyper-parameters. The grey wolf count is set as the initial position of solutions, as expressed as,

$$J_{kl}; (1 \leq k \leq \varsigma); (1 \leq l \leq \rho) \qquad (24)$$

where, ς represents the total grey wolf and ρ is the location of the grey wolf in the coordinate axis.

ii) Calculation of fitness measure: The fitness measure is found using the factors, such as precision, accuracy, and recall measures, which are expressed as,

$$F = \left(\frac{Accuracy + precision + recall}{3} \right) \qquad (25)$$

The value of fitness must be maxima for the solution to be optimal in such a way as to enhance the effectiveness of the proposed mango leaf disease classification module.

iii) Evaluation of best solution: The best solution is considered as L, MT grey wolf depending on their corresponding fitness measure, which is maximal over all the iterations. Once the best outcome is found, the other grey wolfs revise their location based on the position of the leader grey wolf.

iv) Update of coefficients: The coefficients used in the optimization algorithm, such as optimization parameters, constants, and random measures are updated to assist the proper stability among exploitation and exploration phases.

v) Stopping condition: The procedure is continued until maximum iterations and the global optimal solution is found. Table 1 demonstrates the pseudocode of the CO-GWO algorithm.

In the proposed work, CO-GWO was employed to tune the hyperparameters of the NN classifier. In tuning of hyperparameters begins with the initialization of the grey wolf population, with each grey wolf representing a specific sequence of hyperparameters. These hyperparameters control the behavior and performance of the NN classifier. The fitness of the CO-GWO was estimated based on the performance metrics such as precision, accuracy, recall, etc., to maximize the fitness value for optimal solutions. The evaluation of the best solution identifies the grey wolf with the highest fitness measure as the leader. Other grey wolves adjust their positions based on the leader's position to explore and exploit promising regions of the hyperparameter search space. Coefficients used in the optimization algorithm, including optimization parameters, constants, and random measures, are updated to maintain a balance between exploitation and exploration. The algorithm continues until a stopping condition, such as reaching a maximum number of iterations, is met. The global optimal solution represents the set of hyperparameters that yield the best performance for the NN classifier. By iteratively applying the CO-GWO optimization algorithm, the hyperparameters of the NN classifier can be properly tuned, enhancing its effectiveness in accurately classifying mango leaf diseases.

4 Results and discussion

The outcomes attained using the CO-GWO-NN mango leaf classification disease module and the comparative evaluation for proving the efficiency of the proposed CO-GWO-NN classifier in mango leaf disease classification are discussed in this part.

4.1 Experimental setup

The analysis is executed in the PYTHON tool set up in Windows 10 OS and 64-bit OS with 16 GB RAM.

4.2 Dataset description

The presented CO-GWO-NN framework was validated with the publically available mango leaf image database collected from the Mendeley data site. This database contains a total of 435 images, out of which 265 images are labeled as diseased and the remaining images are normal mango leaves.

Table 1 Pseudocode of CO-GWO algorithm

Sl. No	**Pseudo code of proposed CO-GWO optimization algorithm**
1	Initialize grey wolf population, and coefficients
2	Calculate the fitness value for the grey wolfs
3	For all ς
4	{
5	J_L as best grey wolf solution
6	J_M as best grey wolf solution
7	J_T as best grey wolf solution
8	}
9	While $t < t_{max}$
10	{
11	Update the grey wolf position as per equation (23)
12	}
13	EndFor
14	Update the coefficients, z, w
15	Evaluate fitness for all grey wolfs
16	Update the solutions $J_{:}, J_M, J_T$
17	$t = t + 1$
18	}
19	End While
20	End For
21	Return J_L^{t+1}

The database was initially split into 412 images for training and 23 images for testing purposes. The training set contains 252 files of diseased images and 161 files of healthy data, and the testing set includes 14 files of disease images and 9 images of healthy files.

Table 2 Sample dataset
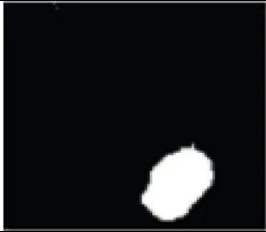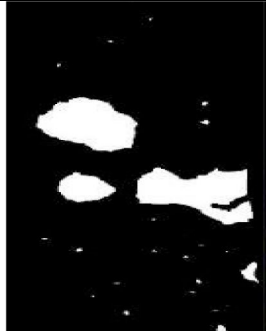
Class	Samples images		
Diseased			
Normal			

Table 3 Image segmentation

Input Images	Segmented Images

The sample of mango leaf images present in the database is tabulated in Table 2. Further, Table 3 illustrates the sample for image segmentation.

4.3 Evaluation metrics

The effectiveness of the CO-GWO-NN module is tested using the metrics described below,

4.3.1 Accuracy

The accuracy is defined as the rate of closeness to the evaluated measure of the system to the real measure of the system, and is expressed mathematically as,

$$Accuracy = \frac{True\ positive + True\ negative}{real\ positive + real\ negative} \qquad (26)$$

4.3.2 Precision

The evaluation of the rate of the total number of true positive values to the sum of true positives and false positives is termed precision, and is expressed as,

$$\Pr ecision = \frac{True\ positive}{True\ positive + False\ positive} \qquad (27)$$

4.3.3 Recall

The term recall is stated as the ratio of true positive values to the number of real positive cases as,

$$\operatorname{Re} call = \left(\frac{True\ positive}{no\ of\ real\ positive\ cases} \right) \qquad (28)$$

4.3.4 F1 measure

The measure of the accuracy of a model is termed the F1 score, and it is the mean of precision and recall.

4.4 Performance analysis

In this section, the performances of the proposed model were analyzed in terms of training percentage and k-fold values. The confusion matrix of the proposed model for the mango leaf image dataset is displayed in Fig. 3. The confusion matrix is a square matrix, which summarizes the performance of a classification model by displaying the counts of true positive, true negative, false positive, and false negative predictions for each class.

By analyzing the confusion matrix, the performance of the classification model is evaluated in terms of accuracy, recall, precision, and f-measure.
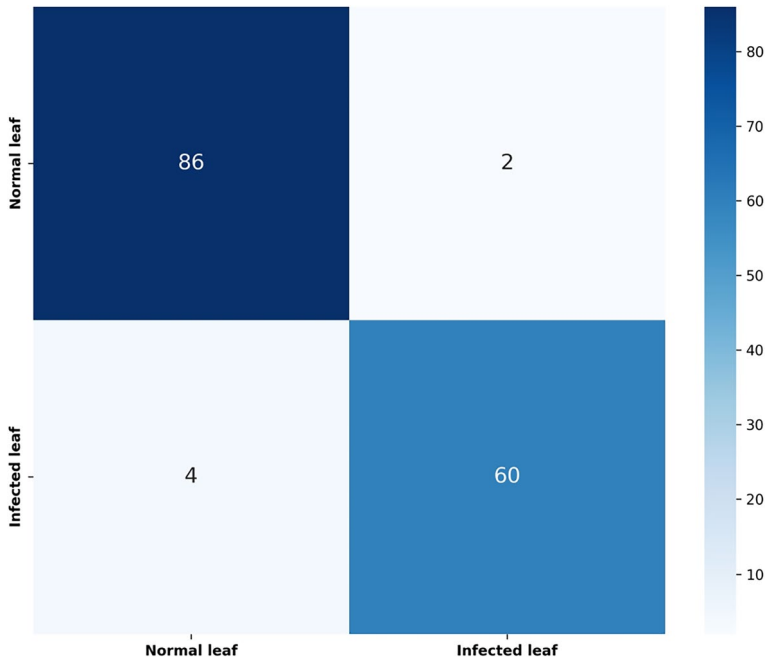
Fig. 3 Confusion matrix

4.4.1 Performance analysis in terms of training percentage

The performances of the presented model were estimated in terms of accuracy, recall, precision, and f-measure by implementing it in Python for the Mango leaf images collected from the Mendeley database. In the proposed work, the outcomes are determined for training percentage and k-fold value. The performances of the designed model were analyzed at different training percentages relative to the number of iterations (epochs). Here, the result parameters are examined at different training percentages as 50%, 60%, 70%, and 80%, respectively by varying the epochs count as 20, 40, 60, 80, and 100. The increase in the performance of the model over increases in epochs demonstrates its efficiency and robustness. When the training data percentage is 50%, the proposed model earned an approximate accuracy of 93.1502%, 93.3832% of precision, 91.5131% recall, and 94.1219% of f-measure over increasing epochs.

Similarly, the system performances were estimated for a 60% training data ratio at varying epoch counts. At 60% training data, the developed model achieved approximate performances of 94.2902% accuracy, 94.5432% precision, 91.5628% recall, and 94.5814% over the increasing number of iterations. Figure 4 illustrates the performances of the system at different training data ratios. Figure 4(a) demonstrates the accuracy of the developed model over epochs at different training data percentages. At 70% training data percentage, the presented model attained approximate outcomes of 94.3132% accuracy, 94.6302% precision, 91.7346% recall, and 95.3086% f-measure. Figure 4(b) displays the precision performance of the system over increasing epochs at different training percentages.
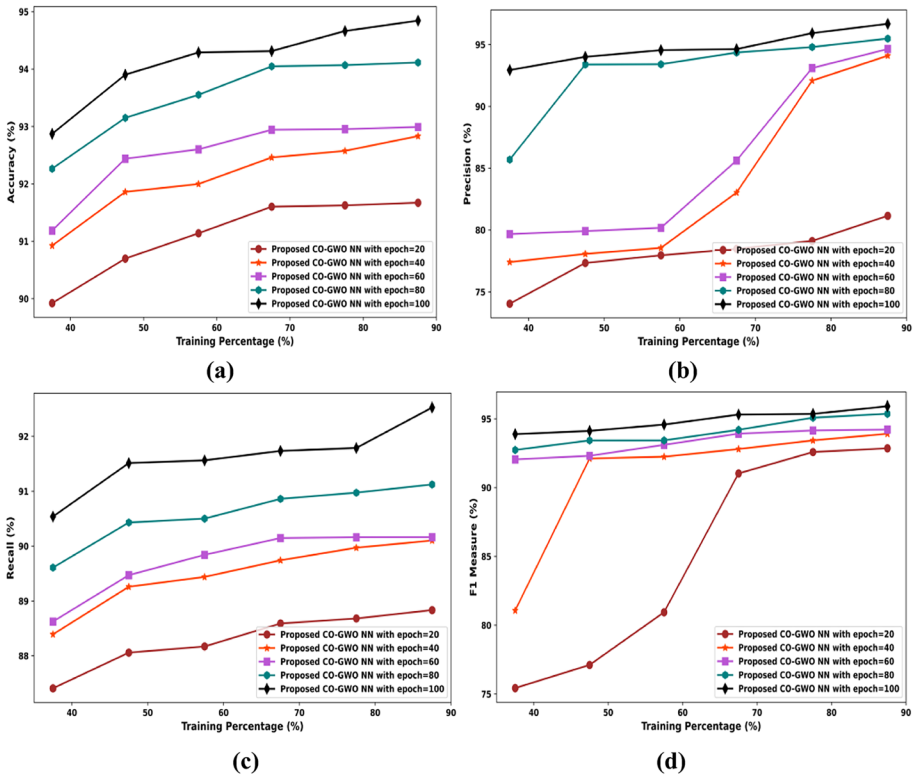
Fig. 4 Performance analysis in terms of training percentage (**a**) accuracy, (**b**) precision, (**c**) recall, and (**d**) F1-measure

Furthermore, the system performances are monitored at an 80% training percentage over increasing epochs. At 80% training percentage, the presented model obtained greater performances such as 94.6627% accuracy, 95.9169% precision, 91.7886% recall, and 95.358% f-measure. Figure 4(c) and (d) represents the recall and f-measure performances of the system at different training percentage with an increasing number of epochs. This comprehensive analysis of system outcomes over increasing epochs at different training percentages illustrates that the performance of the presented model was improved over the increase in epochs and training percentage.

4.4.2 Performance analysis in terms of k-fold value

In this section, the performances of the proposed CO-GWO-NN framework were analyzed at different k-fold values over increasing epochs. Figure 5 portrays the system performances at different k-fold values as 2, 4, 8, and 10 with increasing numbers of iterations as 20, 40, 60, 80, and 100. For a k-fold value of 2, the designed model achieved performances of 90.9905% accuracy, 90.3260% precision, 90.2493% recall, and 90.4388% f-measure over increasing epochs. Figure 5(a) illustrates the accuracy of the system over increasing epochs at different k-fold values. For the k-fold value of 4, the designed model attained an approximate accuracy of 91.5318%, precision of
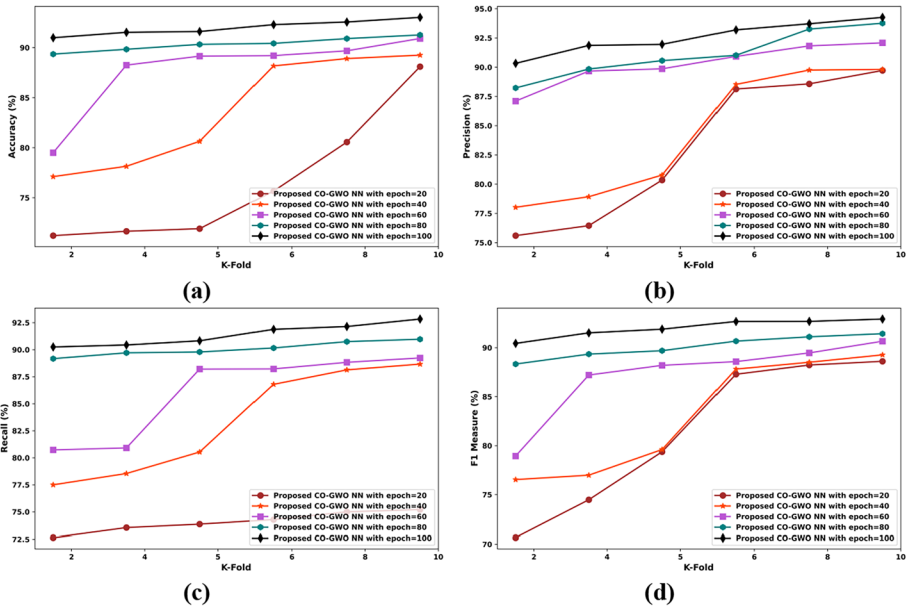
Fig. 5 Performance analysis in terms of k-fold value (**a**) accuracy, (**b**) precision, (**c**) recall, and (**d**) F1-measure

91.859%, recall of 90.4364%, and f-measure of 91.5146%. Figure 5(b) demonstrates the precision of the system at varying k-fold values over increasing epochs. Similarly, the system performances are examined fog k-fold value of 8.

For the k-fold value of 8, the presented framework earned approximately 92.5632% accuracy, 93.7122% precision, 92.1433% recall, and 92.685% f-measure with increasing the epochs. Figure 5(c) displays the recall performances of the system for different k-fold values over epochs. Finally, the presented model outcomes are analyzed for the k-fold value of 10 over an increasing number of epochs as 20, 40, 60, 80, and 100. For the k-fold value of 10, the developed CO-GWO-NN framework obtained performances of 93.0279% accuracy, 94.2601% precision, 92.8359% recall, and 92.9251% f-measure. Figure 5(d) represents the f-measure of the designed model for different k-fold values over the increasing number of epochs. The increase in system performances over the increase in k-fold value and epochs demonstrates the effectiveness of the proposed approach.

4.5 Comparative evaluation

This section deliberates the comparative evaluation of techniques in terms of k-fold and training percentage. The strategies considered for comparison with the proposed CO-GWO-NN are the K-nearest neighbor classifier [34], SVM classifier [35], Neural network (NN) [34], COA-NN [33, 34], and the GWO-NN [32, 36].
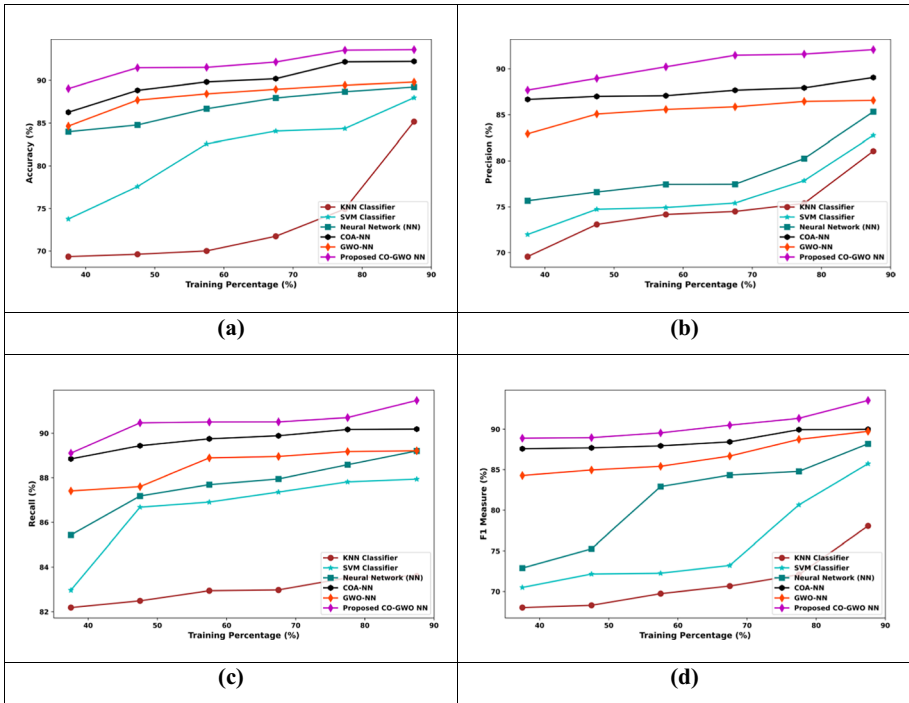
Fig. 6 Performance evaluation in terms of training percentage (**a**) accuracy, (**b**) precision, (**c**) recall, and (**d**) F1-measure

4.5.1 Comparative analysis in terms of training percentage

In this module, the performances of different existing techniques are compared with the proposed model for validation purposes. The performances of the conventional approaches such as K-NN, SVM, NN, COA-NN, and GWO-NN are validated with the presented model. The comparison of the proposed model performance relative to the training percent is portrayed in Fig. 6. At 50% training percent, the traditional models such as K-NN, SVM, NN, COA-NN, GWO-NN, and the developed model attained an approximate accuracy of 70%, 77.5%, 85%, 89%, 88%, and 91% respectively. At 60% training percent, these models achieved an approximate accuracy of 70.0128%, 82.5%, 87%, 90%, 88%, and 91.5%, respectively. Similarly, at 70% training percent the existing models such as K-NN, SVM, NN, COA-NN, GWO-NN, and the presented approach obtained an approximate accuracy of 72%, 84%, 88%, 90%, 89%, and 92%, respectively. Furthermore, the performances of the methods such as K-NN, SVM, NN, COA-NN, GWO-NN, and the presented CO-GWO-NN model were analyzed at 80% training percent. At 80% training percent, these models earned accuracy of 75%, 84%, 89%, 92%, 89%, and 93.5%, respectively. Figure 6(a) illustrates the accuracy of various models at different training percentages.

Consequently, the other performance parameter like precision was compared with existing models. Figure 6(b) demonstrates the comparison of the precision of different techniques. At 50% training percent, the methods like K-NN, SVM, NN, COA-NN, GWO-NN, and the designed CO-GWO-NN technique earned an approximate precision of 73%, 75%,

77%, 87%, 85%, and 89% respectively. Similarly, at 60% training percent these models achieved an approximate precision of 74%, 75%, 77%, 87%, 85.5%, and 90%, respectively. For 70% training percentage, the techniques such as K-NN, SVM, NN, COA-NN, GWO-NN, and the proposed approach attained an approximate precision of 74%, 75%, 77%, 88%, 86%, and 91%, respectively. Finally, for the 80% training percent, the models including K-NN, SVM, NN, COA-NN, GWO-NN, and the GWO-NN model earned an approximate precision of 75%, 76%, 80%, 88%, 86%, and 92%, respectively.

Figure 6(c) portrays the comparison of recall performance of various models at different training percent. For 50% training percentage, the methods such as K-NN, SVM, NN, COA-NN, GWO-NN, and CO-GWO-NN obtained an approximate recall percentage of 82%, 87%, 87%, 89%, 88%, and 90% respectively. For a 60% training percentage, the above-mentioned models attained an approximate recall rate of 83%, 87%, 88%, 90%, 89%, and 90.5%, respectively. On the other hand, for 70% training percentage these techniques achieved an approximate recall of 82%, 87%, 88%, 90%, 89%, and 90.5%, respectively. Finally, the performance of different models at 80% training percentage was validated. The approaches like K-NN, SVM, NN, COA-NN, GWO-NN, and CO-GWO-NN earned an approximate recall rate of 83%, 88%, 88.5%, 90%, 89%, and 91%, respectively.

The comparative performance of the f-measure relative to different training percentages is illustrated in Fig. 6(d). The models such as K-NN, SVM, NN, COA-NN, GWO-NN, and CO-GWO-NN attained an approximate f-measure of 68%, 72%, 75%, 88%, 85%, and 89% respectively for 50% training percentage. For a 60% training percentage, the above-mentioned techniques earned f-measure of 70%, 72%, 83%, 88%, 85%, and 89.5%, respectively. For 70% training percentage, the techniques such as K-NN, SVM, NN, COA-NN, GWO-NN, and CO-GWO-NN obtained f-measure of 71%, 73%, 84%, 88%, 87%, and 90.5%, respectively. Finally, the f-measure performance was examined at 80% training percentage was evaluated. The methods like K-NN, SVM, NN, COA-NN, GWO-NN, and CO-GWO-NN achieved f-measure of 72%, 81%, 85%, 90%, 89%, and 91%, respectively. This intensive comparative analysis demonstrates that the developed model outperformed the existing models in terms of accuracy, precision, recall, and f-measure. This illustrates the integration of multiple approaches into a single CO-GWO-NN model enhances the disease classification performances.

4.5.2 Comparative analysis in terms of k-fold value

The comparative performance of various models relative to different k-fold values is illustrated in Fig. 7. Figure 7(a) demonstrates the accuracy outcomes of the approaches for different k-fold values. At different k-fold values ((2, 4, 5, and 8), the models such as K-NN, SVM, NN, COA-NN, GWO-NN, and the proposed CO-GWO-NN achieved an average accuracy of 79%, 82%, 88%, 95%, 90%, and 97%, respectively. Figure 7(b) portrays the comparison of precision percentages in terms of different k-fold values. For the varying k-fold values, the methods including K-NN, SVM, NN, COA-NN, GWO-NN, and the developed CO-GWO-NN earned approximately an average precision rate of 80%, 85%, 90%, 97%, 95.5%, and 97.5%, respectively.

Similarly, the recall rates of different models are evaluated in terms of k-fold values in Fig. 7(c). The existing techniques like K-NN, SVM, NN, and COA-NN obtained an average recall rate of 82%, 83%, 84%, 95%, and 95%, respectively. But the proposed model attained a greater recall rate of 97%, which is higher than the existing models. Furthermore, the f-measure performances of different existing models and the proposed model were
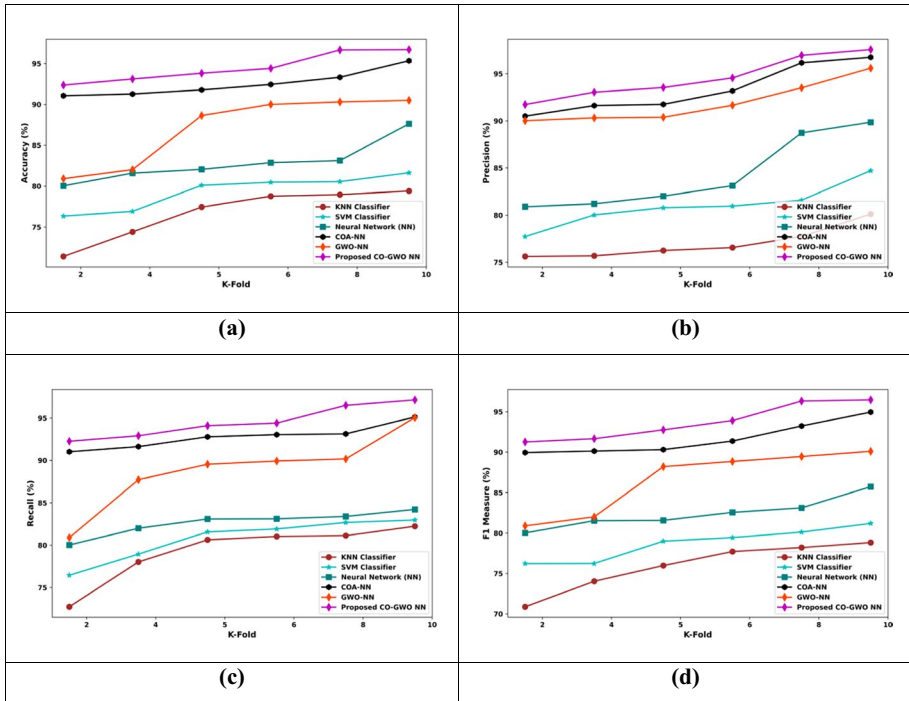
Fig. 7 Performance evaluation in terms of k-fold value (**a**) accuracy, (**b**) precision, (**c**) recall, and (**d**) F1-measure

evaluated in terms of k-fold value. Figure 7(d) displays the evaluation of the f-measure of different techniques relative to the k-fold value. The existing techniques such as K-NN, SVM, NN, and COA-NN obtained f-measure of 79%, 81%, 86%, 95%, and 95%, respectively. However, the designed model attained a higher f-measure of 97%, which is greater than the f-measure attained by the existing models. This intensive evaluation of system performances with existing approaches validates the efficiency of the proposed model.

4.5.3 Comparison with state-of-art techniques

Furthermore, to manifest the effectiveness and robustness of the proposed model, the average system performances are compared within recent state-of-art techniques such as ESDNN, HDL-SVM, ORNN, DCGAN, CNN, LCNN, and VGGNet16. The average performances earned by the presented model such as accuracy, recall, precision, and f-measure are compared with the above-mentioned techniques. The comparison of presented model performances with state-of-art models is illustrated in Fig. 8. Figure 8(a) demonstrates the comparison of system accuracy with different models. The existing models including ESDNN, HDL-SVM, ORNN, DCGAN, CNN, LCNN, and VGGNet19 attained accuracy of 86.108%, 85.432%, 87.954%, 85.870%, 88.754%, 89.912%, and 86.921%, respectively. The average accuracy earned by the designed model is 95.592%, which is greater compared to the state-of-art approaches. Figure 8(b) displays the comparison of recall performance. The performances of these techniques are estimated for the mango leaf database.
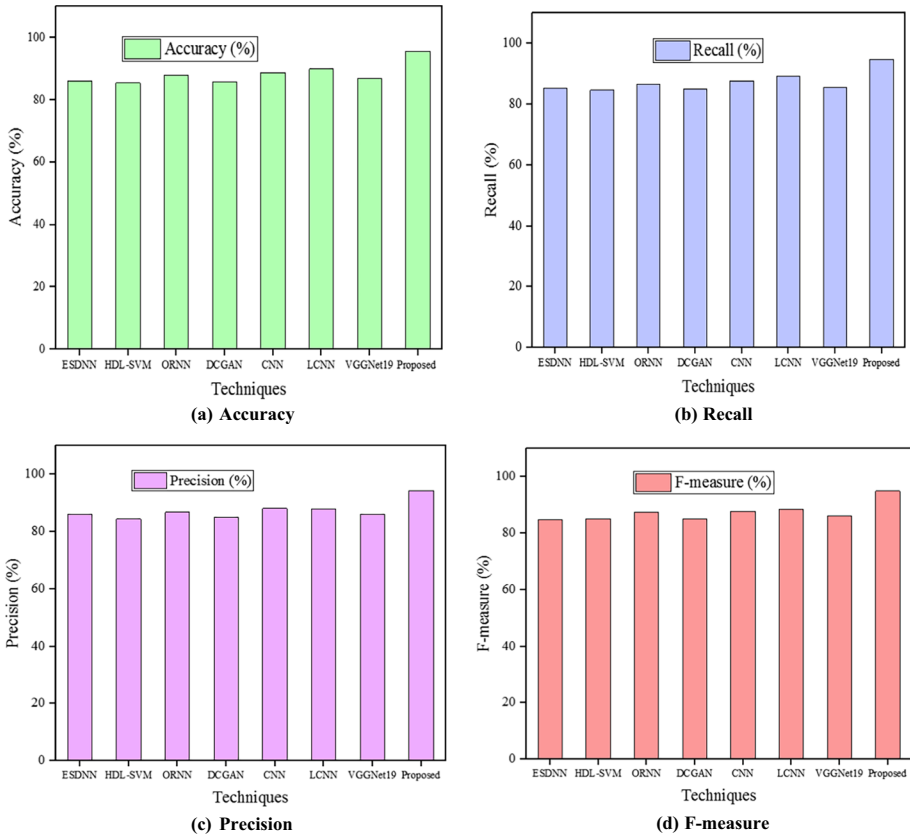
Fig. 8 Comparative analysis: (**a**) Accuracy, (**b**) Recall, (**c**) Precision, and (**d**) F-measure

The state-of-techniques such as ESDNN, HDL-SVM, ORNN, DCGAN, CNN, LCNN, and VGGNet19 obtained the recall of 85.192%, 84.710%, 86.543%, 85.120%, 87.652%, 89.215%, and 85.432%, respectively. But the proposed model earned a higher recall of 94.834%, which is greater than the state-of-art models. Figure 8(c) portrays the comparison of the precision of different models. The state-of-art approaches such

Table 4 Statistical comparative analysis with state-of-art models

Techniques	Accuracy	Recall	Precision	F-measure
ESDNN	86.108	85.192	85.938	84.761
HDL-SVM	85.432	84.710	84.395	85.075
ORNN	87.954	86.543	86.762	87.405
DCGAN	85.870	85.120	84.970	85.032
CNN	88.754	87.652	88.065	87.771
LCNN	89.912	89.215	88.045	88.573
VGGNet19	86.921	85.432	86.109	86.170
Proposed	95.592	94.834	94.3113	95.0119

as ESDNN, HDL-SVM, ORNN, DCGAN, CNN, LCNN, and VGGNet19 attained precision percentages of 85.938%, 84.395%, 86.762%, 84.970%, 88.065%, 88.045%, and 86.109%, respectively. The implementation of the proposed model earned 94.3113% recall, which is higher than the state-of-art models. Figure 5(d) demonstrates the f-measure comparison.

The proposed model earned an excellent f-measure of 95.0119%. On the other hand, the state-of-art models such as ESDNN, HDL-SVM, ORNN, DCGAN, CNN, LCNN, and VGGNet19 obtained greater f-measure of 84.761%, 85.075%, 87.405%, 85.032%, 87.771%, 88.573%, and 86.170%, respectively. The numerical comparative analysis is illustrated in Table 4. This intensive comparative analysis demonstrates that the presented model achieved greater disease classification compared to the recent state-of-art models.

4.6 Discussion

In this article, a novel hybrid disease classification strategy was designed to predict the normal and infected mango leaves. This method employs the CO-GWO approach to optimize the classification process. The presented model was trained and tested with the mango leaf images collected from the Mendeley database and the performances are evaluated. Furthermore, a comprehensive comparative analysis was performed with different existing models in terms of training percentage and k-fold value. In addition, to evaluate the effectiveness of the developed model the system performances are compared with the state-of-art techniques. This intensive performance analysis demonstrates that the developed model outperformed the existing techniques in terms of accuracy, precision, recall, and f-measure. Table 5 presents the overall comparative analysis of different models in terms of training percentage and k-fold value.

Table 5 Comparative discussion

S.No	Evaluation means	Metrics	Methods					
			K-NN	SVM	NN	COA-DCNN	GWO-DCNN	Proposed CO-GWO-NN
1	Training percentage	Accuracy (%)	85.1657	87.9742	89.2238	92.2329	89.8044	93.6147
		Precision (%)	81.0686	82.7593	85.3350	89.0536	86.5736	92.0977
		Recall (%)	83.6094	87.9421	89.2053	90.1873	89.2123	91.4722
		F1-measure	78.0563	85.7318	88.1936	89.9884	89.7375	93.5446
2	K-fold value	Accuracy (%)	79.4041	81.6254	87.6198	95.3420	90.4980	96.7111
		Precision (%)	80.1231	84.7131	89.8507	96.7548	95.5976	97.5712
		Recall (%)	82.2482	82.9813	84.2290	95.1290	95.0526	97.1504
		F1-measure	78.8264	81.2042	85.7380	94.9616	90.0989	96.4792

5 Conclusion

This research article proposes a hybrid optimization strategy for mango leaf disease categorization with the aid of the images extracted from Mendeley data. In specific, the Coyote-Grey wolf optimization (CO-GWO) algorithm involves the optimal tuning of the parameters of the neural network (NN) classifier, which involves the classification process through the features extracted from the input image. The proposed CO-GWO algorithm is important in the enhancement of the efficiency of the proposed classification model as it considers the best weights of the NN classifier. The efficiency of the CO-GWO-NN strategy is analyzed with the evaluation indices, namely accuracy, recall, precision, and F1-measure, which are attained to be 96.7111%, 97.5712%, 97.1504%, and 96.4792%, respectively. This ensures the dominance of the developed strategy's ineffective classification when evaluated against the conventional methods. In the future, an ensemble classifier will be utilized to further boost the accuracy of the proposed model of mango leaf disease classification.

Data availability Data sharing is not applicable to this article as no new data were created or analyzed in this study.

Code availability Not applicable

Declarations

Conflict of interest The authors declare that they have no conflict of interest.

Consent to participate Not applicable

Consent for publication Not applicable

Human and animal rights This article does not contain any studies with human or animal subjects performed by any of the authors.

Informed consent Informed consent does not apply as this was a retrospective review with no identifying patient information.

References

1. Mutengwa CS, Mnkeni P, Kondwakwenda A (2023) Climate-smart agriculture and food security in Southern Africa: a review of the vulnerability of smallholder agriculture and food security to climate change. Sustainability 15(4):2882
2. Bhadra S, Dyer AR (2022) Resilience and well-being among the survivors of natural disasters and conflicts. Handbook of health and well-being: challenges, strategies and future trends. Singapore: Springer Nature Singapore, pp 637–667
3. Chakma S et al (2022) Adapting land degradation and enhancing ethnic livelihood security through fruit production: Evidence from hilly areas of Bangladesh. Agro-biodiversity and Agri-ecosystem Management. Singapore: Springer Nature Singapore 217-238
4. Kumar, P et al (2023) Achieving biodiversity conservation, livelihood security and sustainable development goals through agroforestry in coastal and island regions of India and Southeast Asia. Agroforestry for sustainable intensification of agriculture in Asia and Africa. Singapore: Springer Nature Singapore, pp 429–486
5. Kandegama WM, Wishwajith W et al (2022) Impacts of climate change on horticultural crop production in Sri Lanka and the potential of climate-smart agriculture in enhancing food security and resilience. Food Security and Climate-Smart Food Systems: Building Resilience for the Global South. Cham: Springer International Publishing, 67–97

6. Gurumita NG, Ramesh GP (2022) Mango leaf disease detection using ultrasonic sensor. IEEE International Conference on Data Science and Information System (ICDSIS). IEEE

7. Rahaman Md et al (2023) A deep learning based smartphone application for detecting mango diseases and pesticide suggestions. Int J Comput Digit Syst 13(1):1–1

8. Molina-Cárdenas L et al (2023) First report of mango malformation disease caused by Fusarium proliferatum in Mexico. Plant Dis 107(2):581

9. Ma Y-W, Chen J-L, Shih C-C (2022) An Automatic and Intelligent Internet of Things for Future Agriculture. IT Professional 24(6):74–80

10. Kumari S, Kumari N (2022) Plant leaf disease identification using machine learning. 11th International Conference on System Modeling & Advancement in Research Trends (SMART). IEEE

11. Garg R, Sandhu AK, Kaur B (2023) A systematic analysis of various techniques for mango leaf disease detection. International Conference on Disruptive Technologies (ICDT). IEEE

12. Mohapatra M et al (2022) Botanical leaf disease detection and classification using convolutional neural network: a hybrid metaheuristic enabled approach. Computers 11(5):82

13. Mohapatra, Madhumini et al (2022) Mango leaf disease detection based on deep learning approach. International Conference on Advancements in Smart, Secure and Intelligent Computing (ASSIC). IEEE

14. Gautam Vinay et al (2023) ESDNN: A novel ensembled stack deep neural network for mango leaf disease classification and detection. Multimed Tools Appl 1–27

15. Jain S, Jaidka P (2023) Mango leaf disease classification using deep learning hybrid model. International Conference on Power, Instrumentation, Energy and Control (PIECON). IEEE

16. Selvakumar A, Balasundaram A (2023) Automated mango leaf infection classification using weighted and deep features with optimized recurrent neural network concept. Imaging Sci J 1–19

17. Mahbub NI et al (2023) Detect bangladeshi mango leaf diseases using lightweight convolutional neural network. International Conference on Electrical, Computer and Communication Engineering (ECCE). IEEE

18. Sharma A, Kaur H, Prashar D (2023) Generative adversarial networks based approach for data augmentation in mango leaf disease detection system. IEEE 12th International Conference on Communication Systems and Network Technologies (CSNT). IEEE

19. Saravanan TM et al (2023) Prediction of mango leaf diseases using convolutional neural network. 2023 International Conference on Computer Communication and Informatics (ICCCI). IEEE

20. Mia MR, Roy S, Das SK, Rahman MA (2020) Mango leaf disease recognition using neural network and support vector machine. Iran J Comput Sci 3(3):185–193

21. Arivazhagan S, Vineth Ligi S (2018) Mango leaf diseases identification using convolutional neural network. Int J Pure Appl Mathematics 120(6):11067–11079

22. Gining RAJM, Fauzi SSM, Yusoff NM, Razak TR, Ismail MH, Zaki NA, Abdullah F (2021) Harumanis mango leaf disease recognition system using image processing technique. IJEECS 23(1):378–386

23. Rajbongshi A, Khan T, Pramanik MMRA, Tanvir SM, Siddiquee NRC (2021) Recognition of mango leaf disease using convolutional neural network models: a transfer learning approach. IJEECS 23(3):1681–1688

24. Rao U, Sanath R, Swathi V, Sanjana L, Arpitha KC, Naik PK (2021) Deep learning precision farming: grapes and mango leaf disease detection by transfer learning. Glob Transit Proceed 2(2):535–544

25. Rao PRK, Swathi K (2020) Mango plant disease detection using modified multi support vector machine algorithm. PalArch's Journal of Archaeology of Egypt/Egyptology 17(7):10567–10577

26. Deeba K, Amutha B (2020) ResNet-deep neural network architecture for leaf disease classification. Microprocess Microsyst 103364

27. Prasetyo E, Adityo RD, Suciati N, Fatichah C (2018) Mango leaf classification with boundary moments of centroid contour distances as shape features. In 2018 International Seminar on Intelligent Technology and Its Applications (ISITIA), pp. 317–320. IEEE

28. Jabid T, Kabir MH, Chae O (2010) Local directional pattern (LDP) for face recognition." In 2010 digest of technical papers international conference on consumer electronics (ICCE), pp. 329–330. IEEE

29. Chakraborti T, McCane B, Mills S, Pal U (2018) Loop descriptor: local optimal-oriented pattern. IEEE Signal Process Lett 25(5):635–639

30. Chouhan SS, Singh UP, Jain S (2020) Web facilitated anthracnose disease segmentation from the leaf of mango tree using Radial Basis Function (RBF) neural network. Wirel Pers Commun 113(2):1279–1296

31. Faris H, Aljarah I, Al-Betar MA, Mirjalili S (2018) Grey wolf optimizer: a review of recent variants and applications. Neural Comput Applic 30(2):413–435

32. Pierezan J, Coelho LDS (2018) Coyote optimization algorithm: a new metaheuristic for global optimization problems. In 2018 IEEE congress on evolutionary computation (CEC), pp. 1–8. IEEE
33. Indriani OR, Kusuma EJ, Sari CA, Rachmawanto EH (2017) Tomatoes classification using K-NN based on GLCM and HSV color space. In 2017 international conference on innovative and creative information technology (ICITech), pp. 1–6. IEEE
34. Kour VP, Arora S (2019) Particle swarm optimization based support vector machine (P-SVM) for the segmentation and classification of plants. IEEE Access 7:29374–29385
35. Kumar SR, Sowrirajan S (2016) Automatic leaf disease detection and classification using hybrid features and supervised classifier. International Journal of Advanced Research in Electrical, Electronics and Instrumentation Engineering 5(6):4556–4563
36. Jhuria M, Kumar A, Borse R (2013) Image processing for smart farming: detection of disease and fruit grading. In 2013 IEEE second international conference on image information processing (ICIIP-2013), pp. 521–526. IEEE